



**HAL**  
open science

## 1-dodecanthiol-assisted aqueous synthesis and characterization of Bi<sub>2</sub>Te<sub>3</sub> nanotubes

Bidur Rijal, Aigerim Baimyrza, Thibault Parein, Quentin Lonne, David Blond, Richard Retoux, Franck Gascoin, Loïc Le Pluart, Cyprien Lemouchi

► **To cite this version:**

Bidur Rijal, Aigerim Baimyrza, Thibault Parein, Quentin Lonne, David Blond, et al.. 1-dodecanthiol-assisted aqueous synthesis and characterization of Bi<sub>2</sub>Te<sub>3</sub> nanotubes. *Nano-Structures & Nano-Objects*, 2021, 25, pp.100629. 10.1016/j.nanoso.2020.100629 . hal-03137196

**HAL Id: hal-03137196**

**<https://hal.science/hal-03137196>**

Submitted on 13 Feb 2023

**HAL** is a multi-disciplinary open access archive for the deposit and dissemination of scientific research documents, whether they are published or not. The documents may come from teaching and research institutions in France or abroad, or from public or private research centers.

L'archive ouverte pluridisciplinaire **HAL**, est destinée au dépôt et à la diffusion de documents scientifiques de niveau recherche, publiés ou non, émanant des établissements d'enseignement et de recherche français ou étrangers, des laboratoires publics ou privés.



Distributed under a Creative Commons Attribution - NonCommercial 4.0 International License

# 1-dodecanthiol-assisted aqueous synthesis and characterization of $\text{Bi}_2\text{Te}_3$ nanotubes

Bidur Rijal<sup>a</sup>, Aigerim Baimyrza<sup>a</sup>, Thibault Parein<sup>a</sup>, Quentin Lonné<sup>a</sup>, David Blond<sup>a</sup>, Richard Retoux<sup>b,\*</sup>, Franck Gascoin<sup>b,\*</sup>, Loïc Le Pluart<sup>a,\*</sup>, Cyprien Lemouchi<sup>a,\*</sup>

a. NORMANDIE UNIV, ENSICAEN, UNICAEN, CNRS, LCMT, 14000 CAEN, FRANCE.

b. NORMANDIE UNIV, ENSICAEN, UNICAEN, CNRS, CRISMAT, 14000 CAEN, FRANCE.

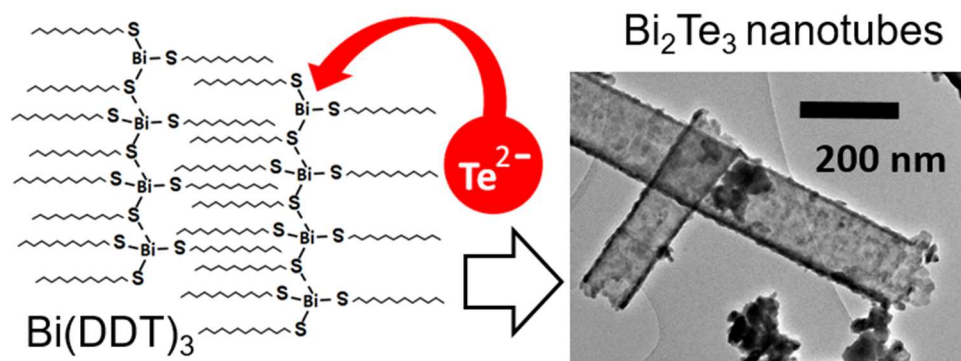
## Corresponding Author

E-mail address: [cyprien.lemouchi@ensicaen.fr](mailto:cyprien.lemouchi@ensicaen.fr) (C. Lemouchi)

LCMT-ENSICAEN, 6 Boulevard Maréchal Juin, 14000 Caen, FRANCE

## Highlights

- A new, scalable and reproducible synthesis of  $\text{Bi}_2\text{Te}_3$  nanotubes was developed
- 200-500 nm long  $\text{Bi}_2\text{Te}_3$  nanotubes were prepared with the assistance of 1-dodecanthiol
- $\text{Bi}_2\text{Te}_3$  tubes length is tuned with the use of a secondary shape-directing agent (SDBS).



For graphical abstract only

## Abstract

This article reports a novel synthetic methodology for preparing  $\text{Bi}_2\text{Te}_3$  nanotubes as well as tailoring their size and aspect ratio, which provides a strong potential interest in the field of thermoelectrics.  $\text{Bi}_2\text{Te}_3$  nanotubes were synthesized via a 1-dodecanethiol (DDT) assisted aqueous two-steps synthesis. One of its main advantages is to be easily scalable because it is carried under mild experimental conditions. The complexation of the capping ligand DDT to the bismuth yields to layered structural

complexes  $\text{Bi}(\text{DDT})_3$ , which may act as a soft templates promoting the growth of  $\text{Bi}_2\text{Te}_3$  nanotubes. The products were characterized by X-Ray Diffraction (XRD), Scanning Electron Microscopy (SEM), Energy Dispersive X-ray analysis (EDX), Transmission Electron Microscopy (TEM) and High-Resolution Transmission Electron Microscopy (HRTEM). Microstructure investigations of powders show that the  $\text{Bi}_2\text{Te}_3$  nanotubes are 200-500 nm long with an average diameter of 50-100 nm. The HR-TEM and selected area electron diffraction (SAED) results reveal the presence of 20-30 nanometers crystallized nanodomains and support the growth of the nanotubes via a rolling up mechanism of (ab) planes. Using sodium dodecylbenzene-sulfonate (SDBS), as an additional structuring agent, lowers the yield of  $\text{Bi}_2\text{Te}_3$  tubes synthesis and increases the heterogeneity of their size distribution. However, with an increased amount of SDBS very long  $\text{Bi}_2\text{Te}_3$  (up to 20  $\mu\text{m}$ ) tubes have been obtained. As a conclusion, using the capping ligand DDT allows obtaining  $\text{Bi}_2\text{Te}_3$  nanotubes in mild conditions according to an easily scalable procedure. Moreover, for the first time the addition of another shape directing agent such as the surfactant SDBS in presence of DDT is shown to be a promising way to tune the dimensions and aspect ratio of these  $\text{Bi}_2\text{Te}_3$  nanotubes, and as a consequence tailor their electronic properties, since the longest hollow  $\text{Bi}_2\text{Te}_3$  tubes ever synthesized have been obtained.

**Keywords:**  $\text{Bi}_2\text{Te}_3$ , nanotubes, capping ligand, structuring agent, X-ray diffraction, scanning electron microscopy (SEM)

## 1-Introduction

As of today, the bismuth telluride  $\text{Bi}_2\text{Te}_3$  [1] and some of its alloys [2,3] are still the most efficient thermoelectric materials [4] for applications running near ambient temperatures and up to 100°C. As a matter of fact, it is the only material used in widespread and well-tried, commercially available converters [5] with the thermoelectric figure of merit (ZT) values comprised between 1 and 2 for both the n and p-type materials [6]. However, a great deal of effort is still devoted to the enhancement of the material efficiency with different strategies. For instance, increasing the texture of polycrystalline materials via multiple pressing or hot forging, making composites by incorporating phonon scatters (carbon nanotubes, refractory metal oxides) or metal doping, have produced promising results [7-9]. Other studies have focused their attention on preparing both highly anisotropic nanosized materials

such as nanoplates, [10-13] nanorods, [14,15] nanowires, [16,17] nanotubes [18-26] or other nanoparticles [27] and phonons scattering materials [12,28]. In this aim, a large number of synthetic techniques like for usual nanoparticles [29,30] have been reported such as hydrothermal [16,19,25], solvothermal [13,31-33] sonochemical [34], micro-wave [10,15,35] synthesis, electrodeposition [20,36] or galvanic displacement [37,38]. Of particular interest is the surfactant-assisted synthesis that uses structuring molecular agents such as hexadecyltrimethylammonium bromine (CTAB) [13,39] sodium dodecylsulfate (SDS) [39], sodium dodecylbenzene-sulfonate (SDBS) [14,16] and TOPO (trioctylphosphine oxide) [40] composed of a hydrophilic head and hydrophobic tail, that favor the growth of particles in a preferential direction thus generating Bi<sub>2</sub>Te<sub>3</sub> nanoplates [39], nanorods [14], nanowires [16]. The type of surfactant and its concentration have a strong impact on the growth step. Recently, the porous and layered nanostructures have attracted attention to enhance the phonons scattering [12]. In this vein, the nanosized Bi<sub>2</sub>Te<sub>3</sub> hollow tubes are gaining widespread interest due to their specific shape which combines two advantages: the anisotropic structure with the preferential growth of (a,b) plan favors a high electrical conductivity, whereas the nanosized grains and the porous architecture are suitable for the phonon scattering, helping to decrease the thermal conductivity. Several reports indicate significant improvement of the ZT of Bi<sub>2</sub>Te<sub>3</sub> when processed from nanotubes rather than from conventional powders [37, 41-43]. Very recently, the work of S. Tadigadapa and *al* even reports measurements on individual nanotubes displaying 11 to 44% increase of Seebeck coefficient (S) (275 to 357  $\mu\text{V K}^{-1}$  at T = 300 K), 64 % decrease of the thermal conductivity ( $\kappa$ ) and a 88 % increase in ZT (ZT=0.75) compared to bulk Bi<sub>2</sub>Te<sub>3</sub> [44].

Several examples of Bi<sub>2</sub>Te<sub>3</sub> nanotubes syntheses have already been reported and various approaches are employed to control the morphology of the particles [18-26,39] among which can be distinguished the hard-templating synthesis using sacrificial nanotubes, nanorods or nanowires with Bi<sub>2</sub>Te<sub>3</sub> tubes formed from the template surface [38,44-52]. In contrast, the soft-templating approach uses structuring molecular agents [39,53]. This technique has drawn attention because it is easily scalable. However, only a few examples are reported. Bi<sub>2</sub>Te<sub>3</sub> nanotubes were prepared from surfactant-assisted wet chemical route with hydrazine hydrate and ethylene glycol in reflux [54] and solvothermal synthesis

[22,23], however, hydrazine hydrate may present a risk for reaction scale up for carcinogenic hazard. On the other hand, hydrothermal syntheses using a capping (complexing) ligand like ethylenediamine-tetra-acetic acid (EDTA) [18,19,24,25,55,56] were developed. For instance Z. Wang [18], Y. Deng [19] and X. B. Zhao [24,25] reported the syntheses of  $\text{Bi}_2\text{Te}_3$  hollow channel tubes with good crystallinity. The role of EDTA as structuring molecular agent in the preparation of nanotubes was emphasized and explained by its bridging nature leading to multinuclear bismuth complexes. Their self-assembly by hydrogen bonding into the lamellar phase favors the nuclei sheets formation and promotes the growth along the (a,b) plane [39,54]. Besides, a second benefit of the capping ligands may be their capacity to slow down the reactivity of tellurium towards bismuth by its complexation to the metal, which promotes anisotropic nanostructures formation. However, these hydrothermal syntheses maybe not suitable for a larger scale because of the volume limitation and the required high temperature and pressure. Hence, the development of a scalable reaction using mild experimental condition appears more attractive for the preparation of thermoelectric materials. In this vein, X. B. Zhao reported a low-temperature wet chemical synthesis with EDTA yielding to  $\text{Bi}_2\text{Te}_3$  nanotubes [24]. The use of other capping (complexing) agents should be interesting in developing alternative scalable syntheses of  $\text{Bi}_2\text{Te}_3$  nanotubes. To the best of our knowledge, no other example of nanotubes wet synthesis with the assistance of another capping (complexing) agent was reported. The 1-dodecanthiol (DDT) is interesting since its complexation to bismuth ions forms multinuclear complexes  $\text{Bi}(\text{DDT})_3$  [57]. The resulting layered structure may act as a soft template promoting the growth of bismuth anisotropic nanostructures as demonstrated in the preparation of nanofilms [57] or nanodisks [58]. In addition, Wu and coworkers [58] highlighted that excessive DDT in Bi nanodisks preparation allows their growth into preferential directions by binding to specific faces of particles.

Hence, in this work, we report a promising scalable synthesis of  $\text{Bi}_2\text{Te}_3$  nanotubes in aqueous solution and mild conditions with the assistance of the capping agent DDT. The nanotubes structure and morphology were characterized by X-Ray Diffraction (XRD), Scanning Electron Microscopy (SEM), Energy Dispersive X-ray analysis (EDX), Transmission Electron Microscopy (TEM), and High Resolution Transmission Electron Microscopy (HRTEM) with selected area electron diffraction

(SAED). The effect of the addition of a secondary shape-directing agent SDBS on the  $\text{Bi}_2\text{Te}_3$  nanotubes morphology has also been investigated in order to open the way to morphology tuning strategies which could help tailoring the electronic properties of those nanotubes.

## 2-Material and methods

### 2-1-Preparation of $\text{Bi}_2\text{Te}_3$ nanotubes

Tellurium (Te, 99.99 %), bismuth (III) chloride ( $\text{BiCl}_3$ , 99.99 %), sodium borohydride ( $\text{NaBH}_4$ , 96 %), sodium hydroxide (NaOH, 98 %), Sodium dodecylbenzenesulfonate (SDBS, 96 %), 1-dodecanethiol (DDT) ( $\text{C}_{12}\text{H}_{25}\text{-SH}$ , 98 %) were purchased from Sigma Aldrich and used as received. De-ionized water and tetrahydrofuran (THF) HPLC grade were degassed by bubbling argon. All the reactions were carried out under argon atmosphere.

The experiment has been carried out in 2L Jacketed stirred reactor vessel, Te(0) (99.99 % purity, 3.47 g, 27.19 mmol, 1 eq.), NaOH (98 % purity, 9.68 g, 237.16 mmol, 8.72 eq.) and  $\text{NaBH}_4$  (96 % purity, 4.18 g, 106.07 mmol, 3.90 eq.) were added successively into 1.3 L of water. The pH was at 13 and the mixture was heated at reflux for 24 h, during the process, the mixture had a pale purple color. In parallel,  $\text{Bi(DDT)}_3$  was prepared by adding 1-dodecanethiol (DDT) (98% purity, 72.2 mL, 61.00 g, 295.84 mmol, 10.88 eq.) to a suspension of  $\text{BiCl}_3$  (99.99 % purity, 5.75 g, 18.23 mmol, 0.67 eq.) in THF (361 mL). After stirring for 24h, the mixture turns into a light yellow homogenous solution. At room temperature, this solution containing  $\text{Bi(DDT)}_3$  and the excess of DDT was added to the  $\text{Te}^{2-}$  containing reaction mixture through a cannula. The mixture was stirred and heated at 70°C up to three days. The obtained black powder (sample A) was filtered and washed successively with water and ethanol, finally dried at 60°C for 6 h, yielding to 7.05g of  $\text{Bi}_2\text{Te}_3$  (8.80 mmol, 97% yield). Samples B and C were prepared following the same procedure, except that SDBS (96 % purity) was added to the mixture just after the  $\text{Bi(DDT)}_3$  solution addition, in various amounts 0.475g (1.33 mmol, 0.05 eq.) for sample B and 0.950g (2.66 mmol, 0.10 eq.) for sample C, the products were obtained with the same yield than for compound A.

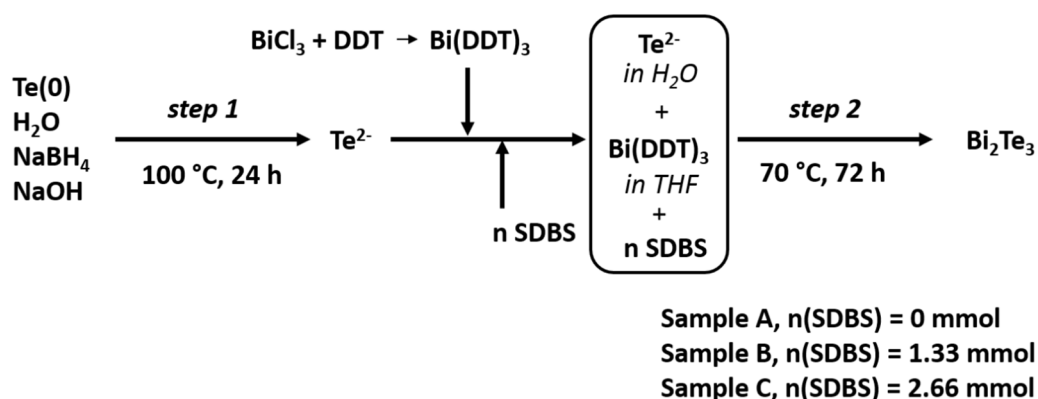
## 2-2-Characterizations

X-ray powder diffraction measurements were carried out on a Panalytical X'Pert Pro diffractometer equipped with an Pixel detector using Cu K $\alpha$  radiation ( $\lambda_{K\alpha 1} = 1.5406 \text{ \AA}$  /  $\lambda_{K\alpha 2} = 1.5444 \text{ \AA}$ ). The data were collected over in 2 theta range  $10^\circ$ – $70^\circ$  and a step size of  $0,0131^\circ$ . The powder microstructure was investigated using a Zeiss Supra 55 Scanning Electron Microscope (SEM) and a JEOL 2010 FEG Transmission Electron Microscope (TEM) operated at 200 kV fitted with a double tilt sample holder for High Resolution observations. Chemical analysis of the sample was investigated by Energy Dispersive Spectroscopy (EDS) analyses performed with EDAX Si/Li detectors fitted on both microscopes. For TEM observations, samples were prepared by dispersing the powder samples in butanol. The flakes in suspension are deposited onto a holey carbon film, supported by a copper grid.

## 3-Results and Discussion

The preparation of Bi<sub>2</sub>Te<sub>3</sub> nanoparticles was carried out in 2 L Jacketed stirred reactor vessel with precise temperature control which enables obtaining 7.00 g of pure Bi<sub>2</sub>Te<sub>3</sub> for each reaction. The aqueous synthesis depicted on Scheme 1 was performed in two steps via an ionic reaction process [59] under argon atmosphere preventing oxidation risks. First, the reduction of tellurium into Te<sup>2-</sup> was performed with NaBH<sub>4</sub> in distilled and degassed water at a pH of 13 under heating at 100°C, during the process, the mixture colored pale purple. For the second step, Bi(DDT)<sub>3</sub> complex was freshly prepared from the reaction with bismuth (III) chloride (BiCl<sub>3</sub>) and DDT in tetrahydrofuran for 24 h. A large excess of DDT was used to prevent oxidation and favor the anisotropic growth of Bi<sub>2</sub>Te<sub>3</sub> particles. The layered structure of Bi(DDT)<sub>3</sub> precursor was checked on the collected yellow powder isolated after evaporation of Bi(DDT)<sub>3</sub> solution and filtration followed by washings with ethanol. The indexation of the diffraction peaks is in good agreement with literature data [57] (see Figure S1, ESI). Then, at room temperature, the solution composed of Bi(DDT)<sub>3</sub> and an excess of DDT was directly added to the Te<sup>2-</sup> containing mixture before heating the reaction mixture at 70°C (Scheme 1). Finally, sample A was collected after 72h. The powder was isolated after filtration, washed successively with water and ethanol, and finally dried at 60°C for 6 h. Bi<sub>2</sub>Te<sub>3</sub> powder was obtained with a yield of 97%

Samples B and C were prepared with the addition at room temperature of 1.33 and 2.66 mmol, of SDBS respectively (Scheme 1).



**Scheme 1.** Schematic two-steps process for the preparation of the samples A, B, and C

Figure 1 depicts the XRD patterns of samples A, B, and C. The indexation of the diffraction peaks is in agreement with the rhombohedral lattice structure of  $\text{Bi}_2\text{Te}_3$  (space group R-3m, JCPDS no. 08-0021). The broadening of diffraction peaks can be attributed to the nanometric size of the crystallites which has been confirmed by TEM observations. No diffraction peak from unreacted Te (0) or any impurities are observed.

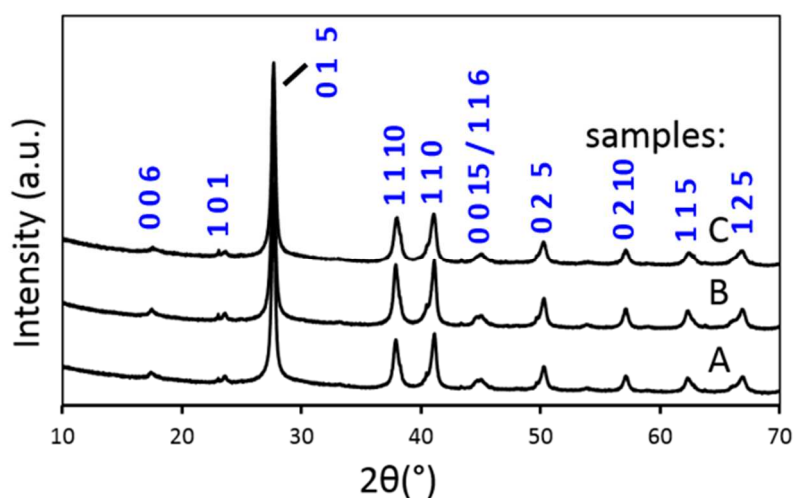


**Figure 1.** X-ray diffraction patterns with the peaks indexation of  $\text{Bi}_2\text{Te}_3$  (space group R-3m, JCPDS no. 08-0021) of the samples A synthesized without SDBS, and the samples B and C with 1.33 and 2.66 mmol of SDBS respectively.



The SEM pictures in Figure 2 show the typical morphology of the sample A particles. The powder is made of micron size particles (Fig 2a). As can be seen on the enlarged picture (Fig 2b) those particles are composed of nanotubes in a proportion of 30 % (Fig 2a, arrow B) packed into a nest-like structure and surrounded by aggregates of isotropic nanoparticles (Figure 2a, arrow A). The opening of the tubes is clearly evidenced (arrow B), characteristic of the hollow tubes similar to reported studies [26]. The length of the tubes varies from 200 to 500 nm. The EDX spectra recorded on the two types of  $\text{Bi}_2\text{Te}_3$  particles and depicted in the inset of Figure 2b indicate that, in each case, the Bi/Te ratios are close to 40/60 in good agreement the expected formula. In addition, the key role played by DDT in the reactivity and in the formation of the nanotubes has been evidenced by preparing sample D in the same conditions (temperature, solvents ...) without DDT. This powder contains mainly  $\text{Te}(0)$  rods and a few aggregates of  $\text{Bi}_2\text{Te}_3$  isotropic particles (X-ray pattern (Figure S2), SEM images (Figures S3, S4 and S5)).

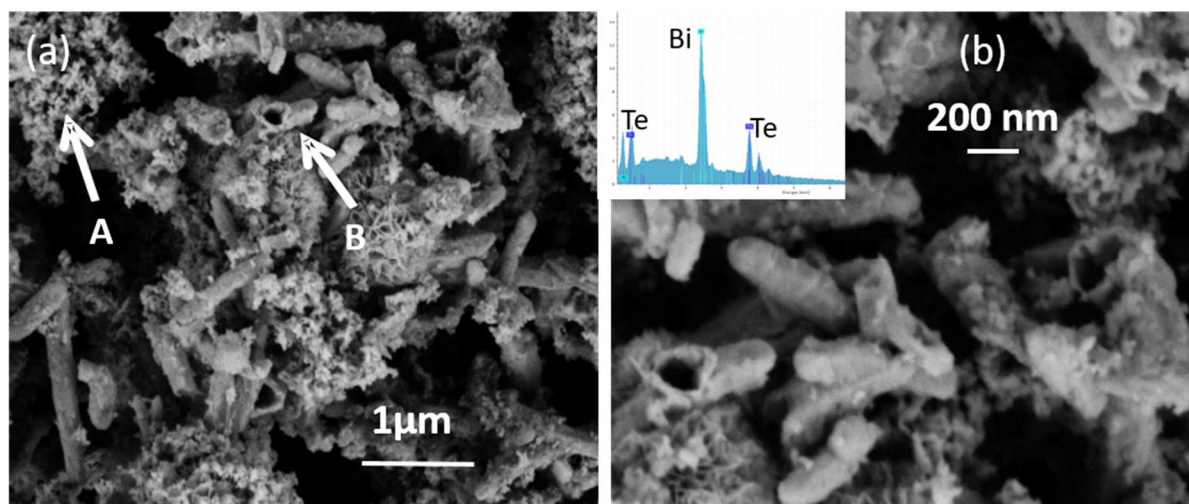


**Figure 2.** Typical SEM images of  $\text{Bi}_2\text{Te}_3$  sample, within inset EDX spectra of the powder (a) blocks of matter are made of two type of  $\text{Bi}_2\text{Te}_3$  crystals, and (b) enlargement evidencing small isotropic  $\text{Bi}_2\text{Te}_3$  nanocrystals aggregated (white arrow A) and open  $\text{Bi}_2\text{Te}_3$  nanotubes (pointed by white arrow B).

TEM was used to investigate more precisely the morphology of these nanoparticles. The TEM picture in Figure 3a shows  $\text{Bi}_2\text{Te}_3$  nanotubes (arrow A) with small nanoparticles aggregates (arrow B). The nanotubes diameter varies from one tube to another but an average value of 50-100 nm can be

estimated. EDX analysis in Figure 3c confirms at the very low scale that the atomic ratio is in agreement with the chemical formula of  $\text{Bi}_2\text{Te}_3$ .

Figures 3a and 3b reveal the specific morphology feature of a hollow tube showing respectively its extended shape along its main axis with spiral walls and the opening of a tube shown on the image taken in its axis. The thickness of the walls is estimated at 20-30 nm. These observations are in agreement with TEM characterizations reported in the literature [18,25,26].

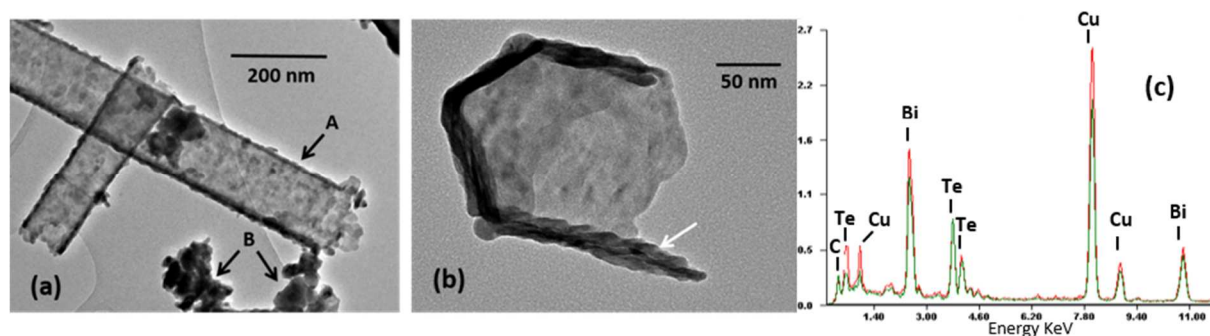


**Figure 3.** (a) TEM pictures of  $\text{Bi}_2\text{Te}_3$  nanotubes and aggregates, (b) zoom on a tube with spiral walls (white arrow), open ends of the tubes are clearly evidenced, and (c) superimposed EDS spectra respectively recorded on nanotubes (A) and aggregates (B)

No differences in the chemical formula can be observed in the two types of  $\text{Bi}_2\text{Te}_3$  shapes. In all cases the Bi/Te ratio deduced from these analyses is close to 2/3, in good agreement with the nominal composition of the samples. On the EDX spectra carbon and copper peaks are systematically observed. These C and Cu contributions are coming from the holey carbon film coated copper grid supporting the observed samples.

In order to further investigate these nanotubes structure, HRTEM analyses have been performed. Figure 4a shows a TEM picture of a representative nanotube. The HRTEM picture in Figure 4b displays the atomic arrangements which evidence the good crystallinity of domains extending over 20-30 nanometers. The contrasts are blurred due to the fact that these small domains are slightly disoriented one to each other, revealing the poly-crystallinity of the tubes. A lot of defects and stacking faults are also clearly evidenced. Although  $\text{Bi}_2\text{Te}_3$  is often referenced with rhombohedral

settings, its description is easier using a hexagonal cell. Indeed, the hexagonal cell is made of layers of atoms stacked perpendicularly to the *c*-axis with the following stacking sequence  $-\text{Te}^1-\text{Bi}-\text{Te}^2-\text{Bi}-\text{Te}^1-$ . The superscript labeling refers and exemplifies the difference of bonding within the quintet, e.g., the  $\text{Te}^2$  layer is bonded to two Bi layers whereas the  $\text{Te}^1$  layer is bonded to Bi on one side and to another  $\text{Te}^1$  layer on the other. The  $\text{Te}^1-\text{Te}^1$  bonding is of Van der Waals type whereas the interaction between Bi and Te is rather ionic-covalent. This 5 layer-sequence is called a quintet and there are 3 quintets per unit cell. The cell parameters are  $a = 4.3835 \text{ \AA}$  and  $c = 30.360 \text{ \AA}$  at 77K [60]. It is, therefore, reasonable to estimate the thickness of a quintet around  $10 \text{ \AA}$ . The measurement in Figure 4b of a distance close to  $10 \text{ \AA}$  along the *c* direction between two bright dots rows corresponds to the thickness of the quintet. The HRTEM observations correlate well with the structural features of  $\text{Bi}_2\text{Te}_3$  crystalline structure. The fast Fourier transform performed in white square area perpendicular to the plane of the wall indicates the average hexagonal orientation of *ab* plane of the crystals (inset in Figure 4a). HRTEM of tube wall endows us to evaluate the *c* parameter close to  $30.4 \text{ \AA}$  (Figure 4b). Figure 4c displays SAED pattern of the sample. The good indexation according to literature data and *hkl* planes identification evidenced the confirmed  $\text{Bi}_2\text{Te}_3$  rhombohedral,  $R(-3)m$  crystalline structure features. Figure 4b also shows that the *c*-axis is not exactly perpendicular to the nanotube axis. This slight disorientation towards that direction is caused by the orientation of the  $\text{Bi}_2\text{Te}_3$  (*ab*) planes from the nanotube wall plane probably caused by their formation via a rolling-up mechanism as previously proposed in the literature [18,56]. The observation of intermediate shapes particles in the powder like nanograin aggregates (Figure 4d) such as sheets (Figure 4d), sheets beginning to roll (Figure 4e) and nanotubes (Figure 4a and 4f) comforts the likeliness of this mechanism.

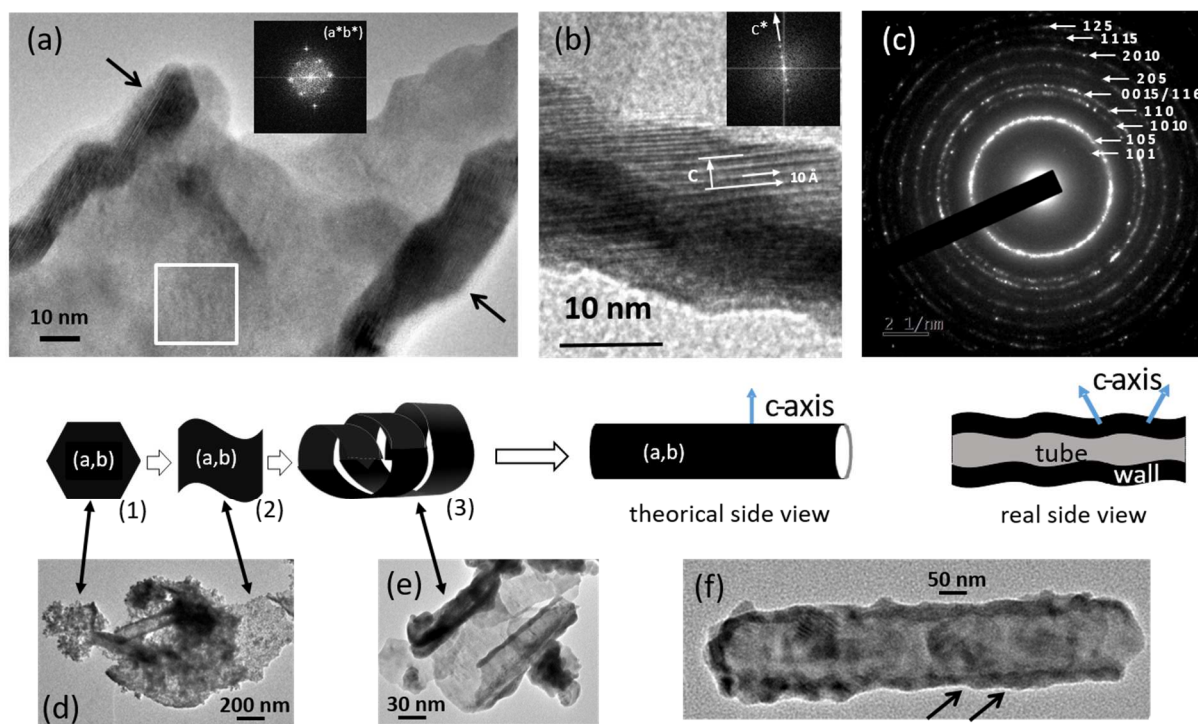


**Figure 4.** (a) and (f) TEM picture of a  $\text{Bi}_2\text{Te}_3$  nanotube with its spiral wall indicated by black arrows; in inset Fast Fourier Transform of the white square area perpendicular to the plane of the wall showing the average hexagonal orientation of the plane of the crystals, (b) HRTEM of a tube wall with white arrows indicating the  $c$  parameter close to  $30.4 \text{ \AA}$  and the basic quintet of  $\text{Bi}_2\text{Te}_3$  (close to  $10 \text{ \AA}$ ) in inset Fast Fourier Transform perpendicular to the wall where the  $C$  axis orientation is clearly evidenced in the wall of the tube, (c) typical SAED diffraction pattern of the  $\text{Bi}_2\text{Te}_3$  aggregates indexed referring to ref [60] parameters. (d), (e) and (f)  $\text{Bi}_2\text{Te}_3$  typical images of respectively nanograin aggregates (d,1), flat sheets (d,2) and sheets beginning to roll (e,3) to form a nanotube (f).

The effect on the nanotubes morphology of adding in the reactive mixture a surfactant (SDBS) to the capping ligand DDT as a second shape-directing agent has been investigated by comparing the structure and morphology of samples A, B and C.

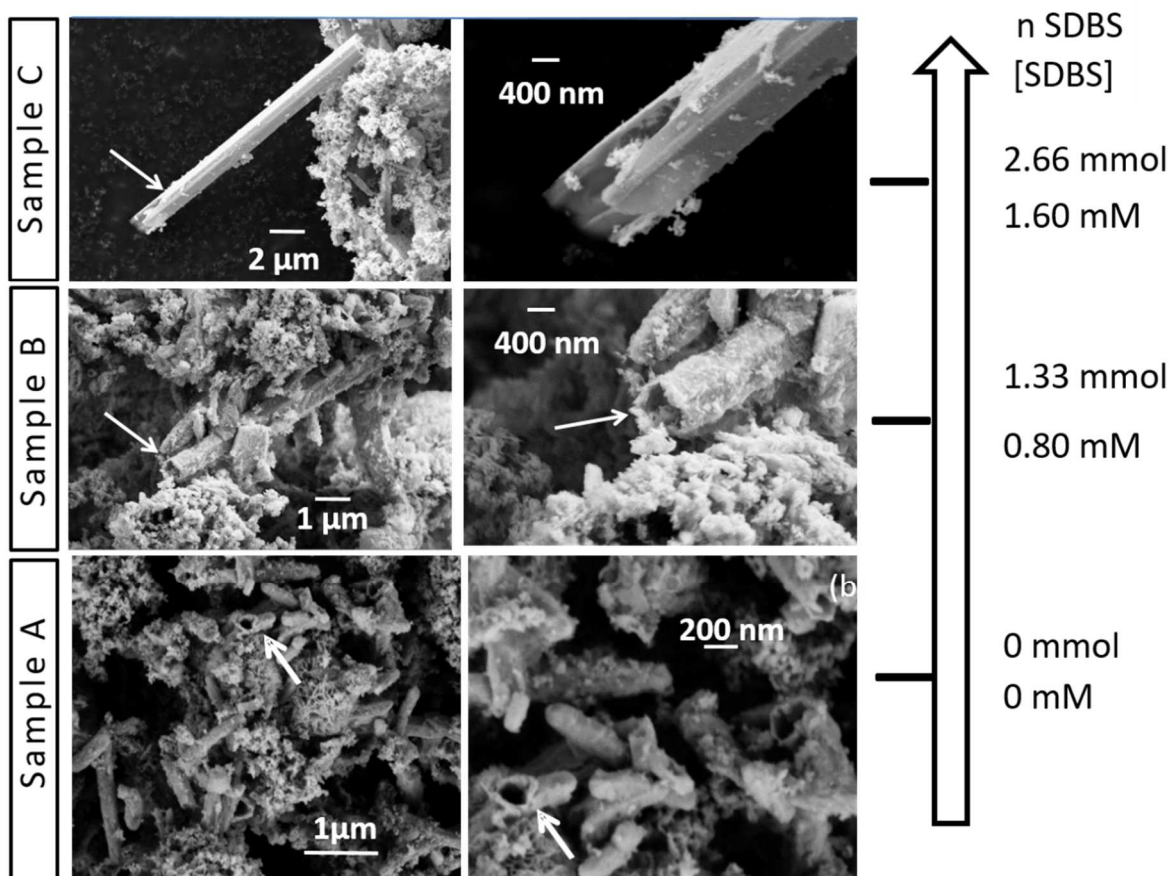


**Figure 5.** SEM images of A, B and C samples respectively prepared with SDBS molar concentrations of 0, 0.80 and 1.60 mM respectively.

The samples B and C were prepared with SDBS molar quantities of 1.33 (0.05 eq.) and 2.66 mmol (0.10 eq.) respectively, which correspond to molar concentrations of 0.80 and 1.60 mM. The powders were analyzed by XRD and the indexation of the diffraction peaks is in agreement with rhombohedral lattice structure  $\text{Bi}_2\text{Te}_3$ . No additional peaks were detected. Figure 5 displays the SEM pictures of the samples A, B, and C. As SDBS concentration increases the quantity of tubes synthesized decreases compared to the quantity of isotropic nanoparticles aggregates obtained. However, with higher molar concentration of SDBS in the preparation, much bigger tubes are obtained. Initially, without SDBS, homogenous size distribution nanotubes were observed with diameters around 50-100 nm and a length varying from 200 to 500 nm. The size distribution is more heterogeneous for samples B and C. This might be explained by the generation of smaller nuclei at high SDBS concentrations and a growth of particles accompanied by more structural defects [14].

For sample B, ([SDBS] = 0.80 mM) the biggest nanotubes observed have a diameter of 200-500 nm (i.e. almost a fivefold increase) and a length of 5-10  $\mu\text{m}$  (i.e. almost a twentyfold increase). For sample C ([SDBS] = 1.60 mM), the diameters are close to 1  $\mu\text{m}$  and the length reaches 15-20  $\mu\text{m}$ , i.e. almost a fortyfold increase. These are the biggest  $\text{Bi}_2\text{Te}_3$  tubes reported in the literature, to the best of our knowledge. This evidences the huge impact that a co-structuring agent can have on the morphology modification of the  $\text{Bi}_2\text{Te}_3$  nanotubes. The combination of the capping ligand and the surfactant may be a way to tune the dimensions of the tubes. However, further investigations are required to determine the optimal proportions between the surfactant and the capping ligand for preparing tubes with a homogenous size distribution.

#### **4-Conclusion**

$\text{Bi}_2\text{Te}_3$  nanotubes were synthesized through an aqueous two-step synthesis with the assistance of the capping ligand DDT. The mild experimental conditions and the easy synthetic process allow the scale-up of the reaction. SEM pictures depicted some aggregates and nanotubes about 50-100 nm in diameter and 200-500 nm in length. XRD and EDX analyses confirm that the obtained nanotubes are composed of  $\text{Bi}_2\text{Te}_3$ . HRTEM pictures reveal the presence of 20-30 nanometers wide crystallized nanodomains in the nanotubes walls. The TEM study of the nanotubes is in good agreement with the structural  $\text{Bi}_2\text{Te}_3$  crystalline structure features (rhombohedral,  $R(-3)m$ ) and support the growth of the nanotubes via a rolling up mechanism favored by a crystalline growth along the (ab) plane. Finally, the effect of an additional structuring agent, the sodium dodecylbenzene-sulfonate on the morphology of the nanoparticles was examined. A reduction in the quantity of synthesized  $\text{Bi}_2\text{Te}_3$  tubes was observed with an increase in their size distribution. In addition, raising the molar concentration of SDBS yields to an increase of the obtained  $\text{Bi}_2\text{Te}_3$  tube dimensions up to 20  $\mu\text{m}$  long, which was never previously reported in the literature. This study evidences the first time the role played by a secondary shape-directing agent SDBS in presence of DDT on particle morphology and demonstrates that there are possibilities to tune the size and aspect ratio of  $\text{Bi}_2\text{Te}_3$  nanotubes, which is a great deal to tailor their electronic properties.

## Acknowledgments

The authors warmly thank the LabEx EMC3 (ANR-10-LABX-09-01) and Normandy Region who supported these research activities through the funding of the ITEM and THEO projects respectively. We also thank the french « ministère de l'enseignement supérieur, de la recherche et de l'innovation », Normandie Université, UNICAEN, ENSICAEN, CNRS, INC3M, ANR, FEDER, LabEx Synorg (ANR-11-LABX-0029), for supporting our research activities. We gratefully acknowledge S. Gascoin from CRISMAT (UMR-CNRS 6508) for XRD measurements on powders.

## Fundings

This work was supported by LabEx EMC3 (ANR-10-LABX-09-01) and Normandy Region through the funding of the ITEM and THEO projects respectively.

## References

- [1] H. J. Goldsmid, Bismuth Telluride and Its Alloys as Materials for Thermoelectric Generation, *Materials* 7 (2014) 2577-2592. <https://doi.org/10.3390/ma7042577>
- [2] L. D. Hicks, M. S. Dresselhaus, Effect of quantum-well structures on the thermoelectric figure of merit *Phys. Rev. B.* 47 (1993) 12727-12731. <https://doi.org/10.1103/PhysRevB.47.12727>
- [3] B. Poudel, Q. Hao, Y. Ma, Y. Lan, A. Minnich, B. Yu, X. Yan, D. Wang, A. Muto, D. Vashee, X. Chen, J. Liu, M. S. Dresselhaus, G. Chen, Z. Ren, High-Thermoelectric Performance of Nanostructured Bismuth Antimony Telluride Bulk Alloys, *Science* 320 (2008) 634-638. DOI: 10.1126/science.1156446
- [4] Y. B. Pottathara , S. Thomas, N. Kalarikkal, Y. Grohens, V. Kokol, *nanomaterials : Nanomaterials Synthesis: Design, Fabrication and Applications*, (2019), Chapter 9, section 9.3. Inorganic thermoelectric Nanomaterials

- [5] L. C. Ding, A. Akbarzadeh, A. Date, Performance and reliability of commercially available thermoelectric cells for power generation, *Applied Thermal Engineering* 102 (2016) 548-556. <https://doi.org/10.1016/j.applthermaleng.2016.04.001>
- [6] M. Saleemi, M. S. Toprak, S. Li, M. Johnsson, M. Muhammed, Synthesis, processing, and thermoelectric properties of bulk nanostructured bismuth telluride ( $\text{Bi}_2\text{Te}_3$ ), *J. Mater. Chem.* 22 (2012) 725-730. <https://doi.org/10.1039/C1JM13880D>
- [7] Q. Lognoné, F. Gascoin, O. Iebedev, L. Lutteroti, S. Gascoin, D. Chateigner, Quantitative Texture Analysis of Spark Plasma Textured n- $\text{Bi}_2\text{Te}_3$ , *Journal of the American Ceramic Society* 97 (2014) 2038-2045. <https://doi.org/10.1111/jace.12970>
- [8] Q. Lognoné, F. Gascoin, Reactivity, stability and thermoelectric properties of n- $\text{Bi}_2\text{Te}_3$  doped with different copper amounts, *Journal of Alloys and Compounds* 610 (2014) 1-5. <https://doi.org/10.1016/j.jallcom.2014.04.166>
- [9] Q. Lognoné, F. Gascoin, On the effect of carbon nanotubes on the thermoelectric properties of n- $\text{Bi}_2\text{Te}_{2.4}\text{Se}_{0.6}$  made by mechanical alloying, *Journal of Alloys and Compounds* 635 (2015) 107-111. <https://doi.org/10.1016/j.jallcom.2015.02.055>
- [10] X. A. Fan, J. Y. Yang, Z. Xie, K. Li, W. Zhu, X. K. Duan, C. J. Xiao, Q. Q. Zhang,  $\text{Bi}_2\text{Te}_3$  hexagonal nanoplates and thermoelectric properties of n-type  $\text{Bi}_2\text{Te}_3$  nanocomposites, *J. Phys. D: Appl. Phys.* 40 (2007) 5975-5979. <https://iopscience.iop.org/article/10.1088/0022-3727/40/19/029>
- [11] M. Hong, T. C. Chasapis, Z.-G. Chen, L. Yang, M. G. Kanatzidis, G. J. Snyder, J. Zou, n-Type  $\text{Bi}_2\text{Te}_{3-x}\text{Se}_x$  Nanoplates with Enhanced Thermoelectric Efficiency Driven by Wide-Frequency Phonon Scatterings and Synergistic Carrier Scatterings, *ACS Nano* 10 (2016) 4719-4727. <https://doi.org/10.1021/acsnano.6b01156>
- [12] M. Hong, Z.-G. Chen, L. Yang, J. Zou, Enhancing thermoelectric performance of  $\text{Bi}_2\text{Te}_3$ -based nanostructures through rational structure design, *Nanoscale* 8 (2016) 8681-8686. <https://doi.org/10.1039/C6NR00719H>



- [13] Y. Xu, Z. Ren, G. Cao, W. Ren, K. Deng, Y. Zhong, Fabrication and characterization of  $\text{Bi}_2\text{Te}_3$  nanoplates via a simple solvothermal process, *Physica B* 404 (2009) 4029-4033. <https://doi.org/10.1016/j.physb.2009.07.153>
- [14] M. Sinduja, S. Amirthapandian, P. Jegadeesan, P. Magudapathy, K. Asokan, Morphological investigations on the growth of defect-rich  $\text{Bi}_2\text{Te}_3$  nanorods and their thermoelectric properties, *CrystEngComm* 20 (2018) 4810-4822. <https://doi.org/10.1039/C8CE00708J>
- [15] Bo Zhou, Yu Zhao, Lin Pu, Jun-Jie Zhu, Microwave-assisted synthesis of nanocrystalline  $\text{Bi}_2\text{Te}_3$ , *Materials Chemistry and Physics* 96 (2006) 192-196. <https://doi.org/10.1016/j.matchemphys.2005.07.010>
- [16] T. Sun, X.B. Zhao, T.J. Zhu, J.P. Tu, Aqueous chemical reduction synthesis of  $\text{Bi}_2\text{Te}_3$  nanowires with surfactant assistance, *Materials Letters* 60 (2006) 2534-2537. <https://doi.org/10.1016/j.matlet.2006.01.033>
- [17] G. Zhang, B. Kirk, L. A. Jauregui, H. Yang, X. Xu, Y. P. Chen, Y. Wu, Rational Synthesis of Ultrathin n-Type  $\text{Bi}_2\text{Te}_3$  Nanowires with Enhanced Thermoelectric Properties, *Nano Lett.* 12 (2012) 56-60. <https://doi.org/10.1021/nl202935k>
- [18] Z. Wang, F.-Q. Wang, H. Chen, L. Zhu, H.-J. Yu, X.-Y. Jian, Synthesis and characterization of  $\text{Bi}_2\text{Te}_3$  nanotubes by a hydrothermal method, *Journal of Alloys and Compounds* 492 (2010) L50-L53. <https://doi.org/10.1016/j.jallcom.2009.11.155>
- [19] Y. Deng, C.-W Cui, N.-L. Zhang, T.-H. Ji, Q.-L. Yang, L. Guo, Fabrication of bismuth telluride nanotubes via a simple solvothermal process, *Solid State Communications*, 138 (2006) 111-113. <https://doi.org/10.1016/j.ssc.2006.02.030>
- [20] G. Zhang, Q. Yu, X. Li, Wet chemical synthesis and thermoelectric properties of V-VI one- and two-dimensional nanostructures, *Dalton Trans.* 39 (2010) 993-1004. <https://doi.org/10.1039/B913462J>

- [21] S. Hyun Kim, B. Ki Park, Solvothermal synthesis of Bi<sub>2</sub>Te<sub>3</sub> nanotubes by the interdiffusion of Bi and Te metals, *Materials Letters* 64 (2010) 938-941. <https://doi.org/10.1016/j.matlet.2010.01.065>
- [22] P. Srivastava, K. Singh, Synthesis and dielectric relaxation behavior of metallic Bi<sub>2</sub>Te<sub>3</sub> nanotubes, *Materials Letters* 108 (2013) 25-28. <https://doi.org/10.1016/j.matlet.2013.06.034>
- [23] P. Kumar, P. Srivastava, J. Singh, R. Belwal, M. K. Pandey, K. S. Hui, K. N. Hui, K. Singh, Morphological evolution and structural characterization of bismuth telluride (Bi<sub>2</sub>Te<sub>3</sub>) nanostructures, *J. Phys. D: Appl. Phys.* 46 (2013) 285301-2855310. <https://iopscience.iop.org/article/10.1088/0022-3727/46/28/285301>
- [24] Y.Q. Cao, T.J. Zhu, X.B. Zhao, Thermoelectric Bi<sub>2</sub>Te<sub>3</sub> nanotubes synthesized by low-temperature aqueous chemical method, *Journal of Alloys and Compounds* 449 (2008) 109-112. <https://doi.org/10.1016/j.jallcom.2006.01.116>
- [25] X. B. Zhao, X. H. Ji, Y. H. Zhang, T. J. Zhu, J. P. Tu, X. B. Zhang, Bismuth telluride nanotubes and the effects on the thermoelectric properties of nanotube-containing nanocomposites, *Appl. Phys. Lett.* 86 (2005) 062111-062113. <https://doi.org/10.1063/1.1863440>
- [26] R. Du, H.-C. Hsu, A. C. Balram, Y. Yin, S. Dong, W. Dai, W. Zhao, D. Kim, S.-Y. Yu, J. Wang, X. Li, S. E. Mohney, S. Tadigadapa, N. Samarth, M. H. W. Chan, J. K. Jain, C.-X. Liu, Q. Li, Robustness of topological surface states against strong disorder observed in Bi<sub>2</sub>Te<sub>3</sub> nanotubes, *physical review B* 93 (2016) 195402-195411. <https://doi.org/10.1103/PhysRevB.93.195402>
- [27] V. R. Akshay, M. V. Suneesh, M. Vasundhara, Tailoring Thermoelectric Properties through Structure and Morphology in Chemically Synthesized n-Type Bismuth Telluride Nanostructures, *Inorg. Chem.* 56 (2017) 6264-6274. <https://doi.org/10.1021/acs.inorgchem.7b00336>
- [28] L. Yang, Z.-G. Chen, M. Hong, G. Han, J. Zou, Enhanced Thermoelectric Performance of Nanostructured Bi<sub>2</sub>Te<sub>3</sub> through Significant Phonon Scattering, *ACS Appl. Mater. Interfaces* 7 (2015) 23694-23699. <https://doi.org/10.1021/acsami.5b07596>

- [29] A. V. Rane, K. Kanny, V. K. Abitha, S. Thomas, Chapter 5, Methods for Synthesis of Nanoparticles and Fabrication of Nanocomposites, Synthesis of Inorganic Nanomaterials Advances and Key Technologies Micro and Nano Technologies (2018), 121-139
- [30] S. Thomas, G. Zaikov, Valsaraj, Meera, Recent, Advances in Polymer Nanocomposites: Synthesis and Characterisation 1st Edition (2010).
- [31] Y. Deng, C W. Nan and L. Guo, A novel approach to  $\text{Bi}_2\text{Te}_3$  nanorods by controlling oriented attachment, Chem. Phys. Lett. 383 (2004) 572-576. <https://doi.org/10.1016/j.cplett.2003.11.090>
- [32] G. Zhang, W. Wang, X. Lu, X. Li, Solvothermal Synthesis of V–VI Binary and Ternary Hexagonal Platelets: The Oriented Attachment Mechanism, Cryst. Growth Des. 9, (2009) 145-150. <https://doi.org/10.1021/cg7012528>
- [33] S. H. Kim, B. K. Park, Solvothermal synthesis of  $\text{Bi}_2\text{Te}_3$  nanotubes by the interdiffusion of Bi and Te metals, Materials Letters 64(8) (2010) 938-941. <https://doi.org/10.1016/j.matlet.2010.01.065>
- [34] Y.Y. Zheng, T.J. Zhu, X.B. Zhao, J.P. Tu, G.S. Cao, Sonochemical synthesis of nanocrystalline  $\text{Bi}_2\text{Te}_3$  thermoelectric compounds, Materials Letters 59 (2005) 2886-2888. <https://doi.org/10.1016/j.matlet.2005.04.035>
- [35] Q. Yao, Y. Zhu, L. Chen, Z. Sun, X. Chen, Microwave-assisted synthesis and characterization of  $\text{Bi}_2\text{Te}_3$  nanosheets and nanotubes, Journal of Alloys and Compounds 481 (2009) 91-95. <https://doi.org/10.1016/j.jallcom.2009.03.001>
- [36] D. Borca-Tasciuc, G. Chen, A. Prieto, M. S. Martin-Gonzalez, A. Stacy, T. Sands, M. A. Ryan, J. P. Fleurial, Thermal properties of electrodeposited bismuth telluride nanowires embedded in amorphous alumina, Appl. Phys. Lett. 85 (2004) 6001-6003. <https://aip.scitation.org/doi/10.1063/1.1834991>
- [37] F. Xiao, B. Yoo, K. Hwan, L. N. V. Myung, Synthesis of  $\text{Bi}_2\text{Te}_3$  Nanotubes by Galvanic Displacement, J. Am. Chem. Soc. 129 (2007) 10068-10069. <https://doi.org/10.1021/ja073032w>

- [38] A. Danine, K. Termentzidis, S. Schaefer, S. Li, W. Ensinger, C. Boulanger, D. Lacroix, N. Stein, Synthesis of bismuth telluride nanotubes and their simulated thermal properties, *Superlattices and Microstructures* 122 (2018) 587-595. <https://doi.org/10.1016/j.spmi.2018.06.042>
- [39] Y. Deng, C.-W. Nan, G.-D. Wei, L. Guo, Y.-H. Lin, Organic-assisted growth of bismuth telluride nanocrystals, *Chemical Physics Letters* 374 (2003) 410-415. [https://doi.org/10.1016/S0009-2614\(03\)00783-8](https://doi.org/10.1016/S0009-2614(03)00783-8)
- [40] B. Kim, S. G. Lee, B. K. Park, Influence of the Capping Agents on Synthesis of Bi<sub>2</sub>Te<sub>3</sub> Nanotubes by Solution-Phase Reaction, *J. Nanosci. Nanotechnol.* 13 (2013) 3568-3572. <https://doi.org/10.1166/jnn.2013.7304>
- [41] H.-T. Zhu, J. Luo, J.-K. Liang, Synthesis of highly crystalline Bi<sub>2</sub>Te<sub>3</sub> nanotubes and their enhanced thermoelectric properties, *J. Mater. Chem. A* 2 (2014) 12821-12826. <https://doi.org/10.1039/C4TA02532F>
- [42] G. Zhang, Q. Yu, W. Wang, and X. Li, Nanostructures for Thermoelectric Applications: Synthesis, Growth Mechanism, and Property Studies, *Adv. Mater.* 22 (2010) 1959–1962. DOI: 10.1002/adma.200903812
- [43] Z. Chai, H. Wang, Q. Suo, N. Wu, X. Wang and C. Wang, Thermoelectric metal tellurides with nanotubular structures synthesized by the Kirkendall effect and their reduced thermal conductivities, *CrystEngComm* 16 (2014) 3507-3514. <https://doi.org/10.1039/C4CE00005F>
- [44] D. Kim, R. Du, S.-Y. Yu, Y. Yin, S. Dong, Q. Li, S. E Mohny, X. Li and S. Tadigadapa, Enhanced thermoelectric efficiency in nanocrystalline bismuth telluride nanotubes, *Nanotechnology* 31 (2020) 365703, <https://doi.org/10.1088/1361-6528/ab97d2>
- [45] S. H. Kim, B. K. Park, Effects of Te nanowire microstructure and Bi<sup>3+</sup>reduction rate on Bi<sub>2</sub>Te<sub>3</sub> nanotubes, *J. Appl. Phys.* 108 (2010) 102808-102812. <https://doi.org/10.1016/j.jieec.2010.07.009>
- [46] H. Y. Kim, M. K. Han, S. J. Kim, Morphological Control of Bi<sub>2</sub>Te<sub>3</sub> Nanotubes and Their Thermoelectric Properties, *J. Nanosci. Nanotechnol.* 15 (2015) 6044-6047. <https://doi.org/10.1166/jnn.2015.10443>

- [47] S. Liu, N. Peng, Y. Bai, H. Xu, D. Y. Ma, F. Ma, K. Xu, General solvothermal approach to synthesize telluride nanotubes for thermoelectric applications, *Dalton Trans.* 46 (2017) 4174-4181. <https://doi.org/10.1039/C7DT00085E>
- [48] Z. Guo, M. Meng, M. Li, J. Wang, S. Huang, Y. Xing, H. Q. Xu, Synthesis of Bi<sub>2</sub>Te<sub>3</sub> Nanotubes Using Te Nanotubes as a Template, *J. Nanosci. Nanotechnol.* 17 (2017) 741-748. <https://doi.org/10.1166/jnn.2017.12683>
- [49] B. Ketharachapalli, N. Nischal Pillala, R. Kishora Dash, Influence of the reducing agent on the formation and morphology of the bismuth telluride nanostructures by using template assisted chemical process: From nanowires to ultrathin nanotubes, *Journal of Crystal Growth* 533 (2020) 125474, <https://doi.org/10.1016/j.jcrysgro.2019.125474>
- [50] S. H. Kim, J. J. Kim, S. W. Suh, B. K. Park, J. B. Lee, The effect of the microstructures of Te nanowires on the crystal growth of one-dimensional Bi<sub>2</sub>Te<sub>3</sub> nanotubes, *Journal of Industrial and Engineering Chemistry* 16(5) (2010) 741-747. <https://doi.org/10.1016/j.jiec.2010.07.009>
- [51] G. Zhang, Qi. Yu, Z. Yao and X. Li, Large scale highly crystalline Bi<sub>2</sub>Te<sub>3</sub> nanotubes through solution phase nanoscale Kirkendall effect fabrication, *Chem. Commun.*(2009) 2317-2319. <https://doi.org/10.1039/B822595H>
- [52] Z. Chai, Z. Peng, C. Wang, H. Zhang, Synthesis of polycrystalline nanotubes Bi<sub>2</sub>Te<sub>3</sub>, *Mater. Chem. Phys.* 113 (2009) 664–669. <https://doi.org/10.1016/j.matchemphys.2008.07.121>
- [53] Y. N. Deng, G.-D. Wei, C.-W. Nan, Ligand-assisted control growth of chainlike nanocrystals, *Chemical Physics Letters* 368 (2003) 639-643. [https://doi.org/10.1016/S0009-2614\(02\)01956-5](https://doi.org/10.1016/S0009-2614(02)01956-5)
- [54] P. Srivastava and K. Singh, Morphological evolution in single-crystalline Bi<sub>2</sub>Te<sub>3</sub> nanoparticles, nanosheets and nanotubes with different synthesis temperatures, *Bull. Mater. Sci.*, 36(5), (2013),. 765–770. <https://doi.org/10.1007/s12034-013-0544-2>
- [55] H. J. Kim, M.-K. Han, H.-Y. Kim, W. Lee, S.-J. Kim, Morphology Controlled Synthesis of Nanostructured Bi<sub>2</sub>Te<sub>3</sub>, *Bull. Korean Chem. Soc.* 33 (2012) 3977-3980. <https://doi.org/10.5012/bkcs.2012.33.12.3977>

- [56] V. R. Akshay, B. Arun, M. V. Suneesh, M. Vasundhara, Surfactant-Induced Structural Phase Transitions and Enhanced Room Temperature Thermoelectric Performance in n-Type Bi<sub>2</sub>Te<sub>3</sub> Nanostructures Synthesized via Chemical Route, ACS Appl. Nano Mater. 1 (2018) 3236-3250. <https://doi.org/10.1021/acsanm.8b00464>
- [57] J. Chen, L.-M. Wu, L. Chen, Syntheses and Characterizations of Bismuth Nanofilms and Nanorhombuses by the Structure-Controlling Solventless Method, Inorg. Chem. 46 (2007) 586-591. <https://doi.org/10.1021/ic0615067>
- [58] Y. Wang, J. Chen, L. Chen, Y.-B. Chen, L.-M. Wu, Shape-Controlled Solventless Syntheses of Nano Bi Disks and Spheres, Crystal Growth and Design 10 (2010) 1578-1584. <https://doi.org/10.1021/cg9010949>
- [59] L. Giri, G. Mallick, A. C. Jackson, M. H. Griep, S. P. Karna, Synthesis and characterization of high-purity, single phase hexagonal Bi<sub>2</sub>Te<sub>3</sub> nanostructures, RSC Adv. 5 (2015) 24930-24935. <https://doi.org/10.1039/C5RA02303C>
- [60] W. Kullmann, J. Geurts, W. Richter, N. Lehner, H. Rauh, U. Steigenberger, G. Eichhorn, R. Geick, Effect of Hydrostatic and Uniaxial Pressure on Structural Properties and Raman Active Lattice Vibrations in Bi<sub>2</sub>Te<sub>3</sub>, Phys. Status Solidi b 125 (1984) 131-138. <https://doi.org/10.1002/pssb.2221250114>